Temperature-independent ytterbium valence in YbGaGe

B. P. Doyle,[1,*] E. Carleschi,[2,1] E. Magnano,[1] M. Malvestuto,[3] A. A. Dee,[4,5,6] A. S. Wills,[4,5] Y. Janssen,[7] and P. C. Canfield[7,8]
[1]*Laboratorio Nazionale TASC, INFM-CNR, S.S. 14, km 163.5, Area Science Park, 34012 Basovizza (TS), Italy*
[2]*Dipartimento di Fisica, Università degli Studi di Trieste, via A. Valerio 2, 34127 Trieste, Italy*
[3]*Sincrotrone Trieste S.C.p.A, S.S. 14 km 163.5, Area Science Park, 34012 Basovizza (TS), Italy*
[4]*Department of Chemistry, University College London, 20 Gordon Street, London, WC1H 0AJ, United Kingdom*
[5]*Davy Faraday Research Laboratory, The Royal Institution of Great Britain, 21 Albemarle Street, London W1S 4BS, United Kingdom*
[6]*Institute Laue-Langevin, 6 rue Jules Horowitz, BP 156, 38042 Grenoble Cedex 9, France*
[7]*Ames Laboratory, Iowa State University, Ames, Iowa 50011, USA*
[8]*Department of Physics and Astronomy, Iowa State University, Ames, Iowa 50011, USA*
(Received 4 November 2006; published 12 June 2007)

We have determined the ytterbium valence as a function of temperature in the reported near-zero thermal expansion material YbGaGe using x-ray photoemission at various incident photon energies. The Yb 3*d*, 4*d*, and 4*f* levels, which directly yield the Yb valence, have been measured. Careful analysis enabled the clear separation of surface and bulk contributions. Resonant photoemission at the 4*d*-4*f* absorption edge was used to enhance the low contribution of the Yb^{3+} component. Contrary to the initially proposed Yb valence transition, we find no change in the valence from room temperature down to 115 K.

DOI: 10.1103/PhysRevB.75.235109 PACS number(s): 65.40.De, 75.30.Mb, 71.20.Eh, 79.60.−i

I. INTRODUCTION

The report of YbGaGe as a near-zero thermal expansion (ZTE) material[1–3] prompted a brief flurry of activity. Salvador and co-workers used x-ray diffraction to determine the cell volume from 100 to 300 K and found it to be nearly constant over this wide temperature range. They suggested an underlying mechanism where, with increasing temperature, a gradual transfer of electrons from the localized Yb 4*f* band to the Ga 4*p* band causes a change in the oxidation state of the Yb from Yb^{2+} to Yb^{3+}. The contraction in the ionic radius of Yb associated with this change in oxidation state compensates for the lattice expansion that would otherwise occur on heating and leads to a net ZTE effect. The same mechanism has been proposed to explain the negative thermal expansion seen in $Sm_{1-x}Gd_xS$,[4] $Sm_{2.75}C_{60}$,[5] $Yb_{2.75}C_{60}$,[6] and $Yb_8Ge_3Sb_5$.[7] In the case of YbGaGe, the authors based their deductions on magnetic susceptibility measurements which show that the Yb magnetic moment changes with temperature (Yb^{3+} is paramagnetic whereas Yb^{2+} is diamagnetic). However, other groups have been unable to duplicate either the ZTE[8–12] or the magnetic susceptibility data supporting the proposed Yb valence transition.[8–13] Instead the magnetic susceptibility was found to be compatible with that of divalent Yb and the thermal expansion to be that of a normal metal. Diffraction measurements on $YbGa_{1.05}Ge_{0.95}$ by a collaboration involving some of the authors of the initial YbGaGe paper revealed no ZTE, instead showing a sudden, large negative thermal expansion at 5 K.[14] This was again proposed to be the result of an Yb valence transition, without, however, the support of magnetic susceptibility measurements.

No direct spectroscopic investigation of the Yb valence as a function of temperature has been reported (Ref. 11 does contain a reference to unpublished photoemission data). X-ray absorption measurements at the Yb L_{III} edge on the nonstoichiometric compound $YbGa_{1.12}Ge_{0.88}$ have been carried out and show the valence to be equal at 5 K and 300 K.[15] Direct determination of the valence is relevant due to the high sensitivity of the magnetic susceptibility to low levels of Yb^{3+}-containing impurities. In particular, groups have found low levels of mixed-valence Yb_3Ge_5 (Refs. 9–11) and trivalent Yb_2O_3 (Ref. 10) in YbGaGe.

We present a synchrotron radiation photoemission study of the Yb valence as a function of temperature. In the rare earths the population of the localized 4*f* levels exactly reflects the valence. Photoemission from the resulting energy levels gives clearly different structures in the spectra for the $4f^{14}(2+)$ and $4f^{13}(3+)$ states.[16] Similarly, due to their strong Coulomb interaction with the 4*f* electrons, and 4*f* holes if present, photoemission of the 3*d* (Refs. 17–19) and 4*d* (Refs. 20 and 21) levels is another clear measure of valence. Spectral weights for a given energy level in photoemission are directly proportional to concentration. Thus the low impurity levels mentioned above give a negligible or small contribution to the spectra.

Low-energy photoemission has been successfully used in many cases to measure rare-earth valence.[22–25] However, some groups report the presence of a subsurface region that possesses different properties from the bulk and consequently adversely affects such surface-sensitive measurements.[25,26] This can result, in selected cases, in temperature-dependent valence transitions appearing broader and of lesser magnitude than when seen with higher photon energies or other techniques.[25,27] There is a general consensus[21,27,28] that energies of the order of Al $K\alpha$ radiation (1486.6 eV) probe the bulk of such materials. This is a result of the increased mean free path and thus escape depth of the photoelectrons at these energies. We have accordingly measured the Yb 4*f* levels at two principal photon energies: one low (182 eV) where higher-resolution data may be more easily taken and the other high (1420 eV) to more clearly probe the bulk.

II. EXPERIMENTAL PROCEDURE

Single crystals of YbGaGe were grown out of a high-temperature ternary solution.[29–31] The initial alloy composition used was $Yb_{0.3}Ga_{0.35}Ge_{0.35}$, and the resulting crystals were well-formed rods. This composition, very close to that of YbGaGe, was chosen because it was found earlier that the desired compound melts congruently,[10] and since congruently melting compounds form part of their own primary solidification, a composition close to the composition of the desired crystals is likely to primarily produce the desired stoichiometric phase.[32] Moreover, the melting temperature that we found earlier, 1193 K,[10] is easily accessible. The starting elements were sealed in a three-cap Ta crucible,[31] in turn sealed in an evacuated quartz ampoule. The ampoule was initially heated up to ≈1470 K to ensure a well-homogenized alloy, then quickly cooled to 1273 K, slightly higher than the melting temperature of YbGaGe, and then slowly cooled down to 1073 K over 100 h. The ampoule was inverted and centrifuged, resulting in a separation of crystals from an excess liquid. X-ray diffraction patterns determined from powdered crystals were consistent with patterns obtained earlier on YbGaGe.[10] The temperature-dependent magnetization below 300 K indicated that the samples yield a smaller magnetization than the polycrystalline YbGaGe, with some 0.5 wt % Yb_2O_3, investigated earlier.[10]

X-ray photoemission measurements were carried out at the BACH beamline[33,34] at the Elettra synchrotron source (Trieste, Italy), using a 150-mm VSW hemispherical electron analyzer. The total energy resolution (photon beam and analyzer) was approximately 55 meV at 72 eV, 80 meV at 165 and 182 eV, 1.5 eV at 1420 eV, and 1.8 eV at 1650 eV. The spectra were normalized to the incident flux. The temperature was measured by a thermocouple placed on the sample holder in close proximity to the samples.

Careful attention was paid to the effect of surface contamination, as Yb is a very reactive element. The samples were cleaved or scraped, depending on dimensions, at room temperature to provide clean surfaces for measurement. The pressure in the chamber was 1.5×10^{-10} mBar which allowed 5–6 h of measurement before a new surface had to be prepared. As oxidation causes an increase in the surface Yb^{3+} component,[35] the valence band at room temperature was used as a measure of the surface cleanliness and remeasured at various stages. The oxygen 1*s* level was also measured but proved to be significantly less sensitive to contamination than the valence band.

III. RESULTS

A. Valence band (low energy)

Figure 1 shows a room-temperature valence-band photoemission spectrum from YbGaGe acquired with a photon energy of 72 eV. The valence band, extending approximately 13 eV from the Fermi level, is dominated by the emission from the Yb states. In particular, the features between the Fermi level and 3.5 eV represent the divalent portion of the Yb signal—i.e., the $4f^{14}\rightarrow4f^{13}$ transition in photoemission—while the trivalent features—i.e., $4f^{13}\rightarrow4f^{12}$—are found between 6 and 13 eV.[16] The peaks lying at a binding energy of approximately 18.5, 23.4, and 28.7 eV correspond, respectively, to the Ga 3*d*, Yb $5p_{3/2}$, and Ge 3*d* core levels. The Yb $5p_{1/2}$ peak is obscured by the much more intense Ge 3*d* line.

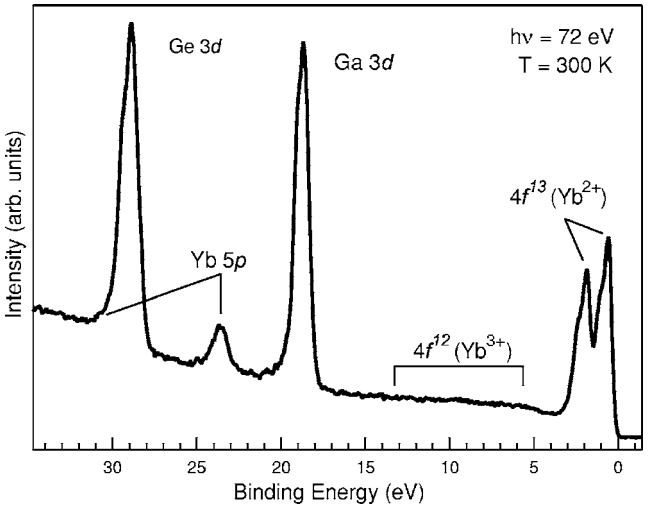

FIG. 1. The valence-band and shallow-core levels of YbGaGe measured at room temperature with a photon energy of 72 eV.

It is clear from Fig. 1 that the valence band in YbGaGe is dominated by the Yb^{2+} component whereas the Yb^{3+} component is rather small. As an accurate determination of the valence requires both components to be precisely measured we have performed resonant photoemission to amplify the Yb^{3+} signal. Here 165 and 182 eV correspond, respectively, to pre- and on-resonance for the $4d\rightarrow4f$ absorption edge for Yb^{3+} states.[35] Using the on-resonance photon energy we obtain an intensity enhancement of the Yb^{3+} valence-band contribution, as a consequence of the quantum interference between two different photoemission channels, the direct photoemission channel $(4f^n+h\nu\rightarrow4f^{n-1}+e_k$, where e_k represents the emitted photoelectron), and the autoionization channel, a photoabsorption process followed by a super-Coster-Kronig Auger decay $(4d^{10}4f^n+h\nu\rightarrow4d^94f^{n+1}\rightarrow4d^{10}4f^{n-1}+e_k)$.[36] Yb^{2+} states do not resonate because in their case the 4*f* shell is fully occupied and photoabsorption cannot take place.

Figure 2 shows the temperature dependence of the valence band (and shallow-core levels) measured between 210 K and 115 K with a photon energy of 182 eV, all taken on the same cleaved surface. In order to find the Yb valence at each temperature we initially analyzed the data following the method outlined in Ref. 21. The upper and lower limits for the spectral weights of the Yb^{2+} and Yb^{3+} contributions were found by integration after subtraction of a minimum and maximum background, respectively. The minimum background is a Shirley background.[37] The maximum background for the Yb^{3+} states consists of two lines which join the minima in the spectra; for the Yb^{2+}, it consists of a single line similarly joining the minima, as in Ref. 21.

As already discussed, the Yb^{3+} part of the spectrum is increased when the photon energy is on-resonance, whereas the Yb^{2+} part is not. The Yb^{3+} on-resonance spectral weights

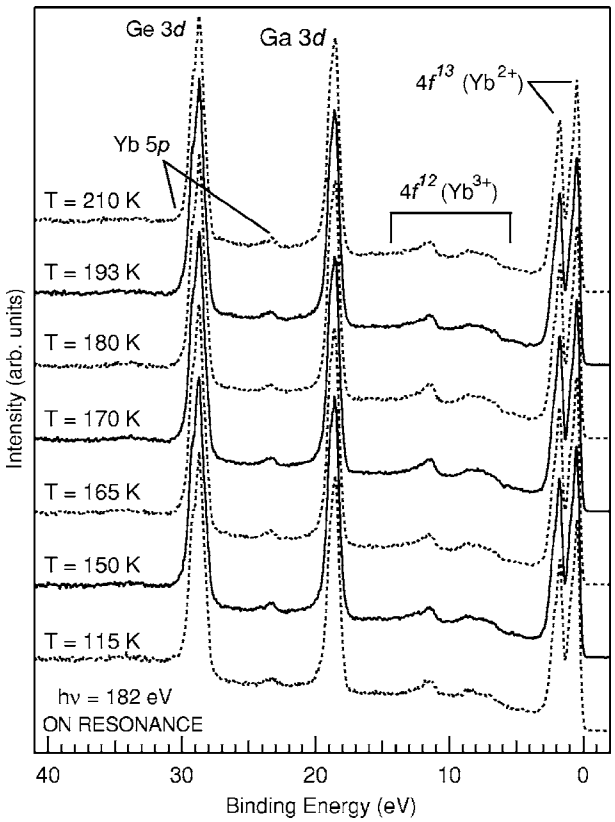

FIG. 2. The valence-band and shallow-core levels of YbGaGe as a function of temperature, measured on-resonance (see text), at 182 eV. All spectra were taken on the same cleaved surface.

must therefore be corrected for this increase before one can calculate the Yb valence. Two spectra were taken under identical experimental conditions, one at 182 eV and the other at 165 eV. The Yb^{3+} spectral weights for each spectrum were then determined using the method outlined above. The ratio of the two values obtained is the correction factor by which all Yb^{3+} spectral weights measured on-resonance must be divided.

The Yb valence v_{Yb}, also expressed as $v_{\mathrm{Yb}}=n_h+2$, where n_h is the hole occupation number, is then directly given by the intensity ratio of the two Yb $4f$ components:[38]

$$n_h = \left(1 + \frac{13}{14}\frac{I_{4f}^{13}}{I_{4f}^{12}}\right)^{-1}. \quad (1)$$

In this way we obtained the two limits for the Yb valence for each spectrum, corresponding to the two different background subtractions. We then calculated the average value with the error bar estimated as half of the range between the two values. The results are plotted in Fig. 3.

If we suppose that, as is the case in many Yb compounds,[23,25,39] the surface is predominantly divalent, then this method incorrectly includes this surface contribution and therefore underestimates the actual valence. We have consequently chosen a more rigorous fitting-based analysis method.

In order to first determine the exact positions of the surface and bulk Yb $4f$ components the valence band was first

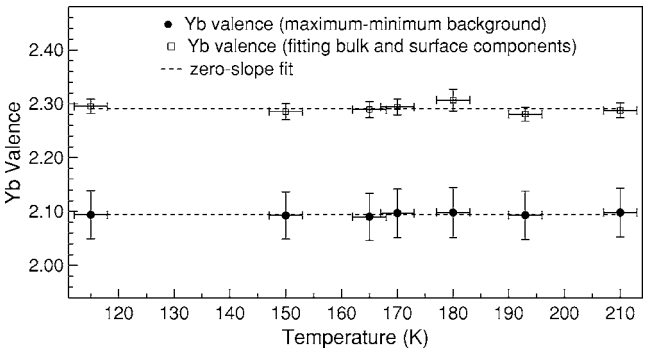

FIG. 3. The Yb valence as a function of temperature, as determined by the two methods in the text, using a photon energy of 182 eV. The dashed lines are zero-slope fits to the data.

measured with a photon energy of 72 eV, chosen so that the electron escape depth is close to the minimum.[23] As such the surface sensitivity is greatly enhanced. Figure 4 shows the Yb^{2+} part of the valence band, taken on both clean and contaminated surfaces. After subtraction of a Shirley background the spectra were fitted with two Doniach-Sunjic doublets, with the spin-orbit splitting being fixed at 1.27 eV and the branching ratio, as expected for f electrons, at 0.75.[23] The fit parameters of the two spectra are consistent within the errors of the fits themselves and serve to fix the position, among other parameters, of the surface component when

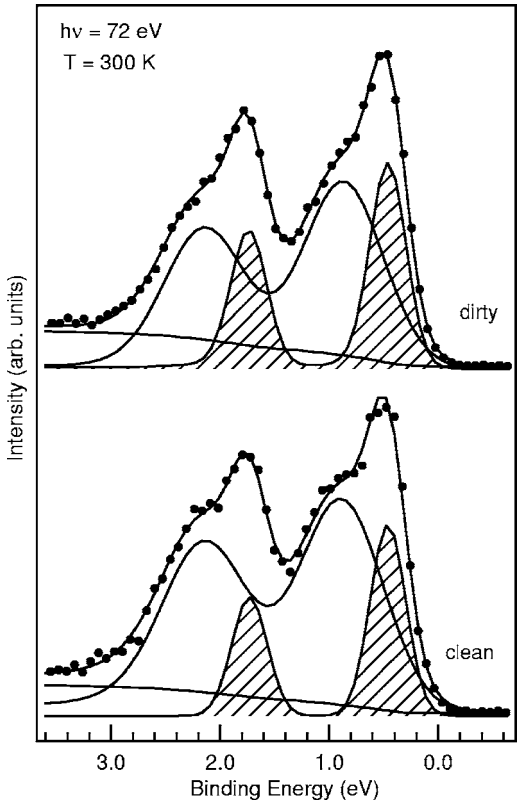

FIG. 4. Determination of the surface and bulk components of the $4f^{13}$ state for clean and contaminated surfaces. The hatched doublet is the bulk component. The surface component is clearly observed to be substantially broader.

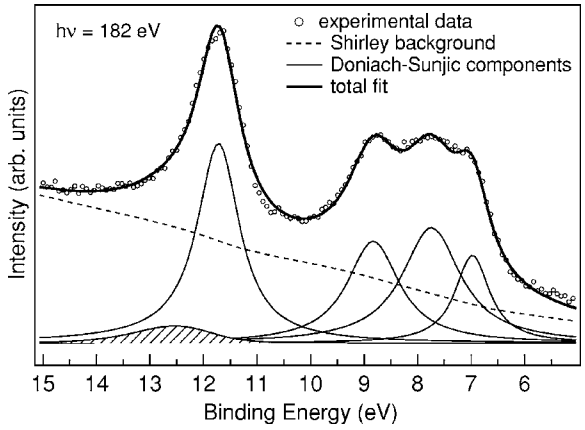

FIG. 5. Fit of the $4f^{12}$ component on an oxidized YbGaGe surface. The hatched peak is that which does not grow upon contamination.

later fitting the valence band at various temperatures. As discussed previously oxidation reduces the surface Yb^{2+} emission and thus the ratio between the Yb^{2+} surface and bulk components. Therefore it is clear from the two spectra that the surface component is that at higher binding energy. This is supported by it having the larger width (see Ref. 39 and references therein) and follows the behavior of other Yb intermetallics which also possess a surface component shifted to higher binding energies.[23,24] We do not resolve a subsurface component, just one from the surface and one from the bulk.

With the information hereby obtained we proceeded, after subtraction of a Shirley background, to fit the temperature-dependent spectra. The Yb^{2+} part was fitted as before at 72 eV, with surface and bulk doublets separated by 0.4 eV, a spin-orbit splitting of 1.27 eV, and a branching ratio of 0.75. The Yb^{3+} component was fitted with five Doniach-Sunjic peaks (initially on a contaminated sample, with its increased 3+ spectral weight, to more easily determine the fit parameters). An example of such a fit is given in Fig. 5.

One of the peaks was found not to increase upon contamination, and we therefore consider it to be some non-$4f$ part of the valence band. As such it was not included in the integration to determine the 3+ spectral weight.

As with the previous method the Yb^{3+} spectral weight has been corrected for the increase due to the $4d$-$4f$ resonance by comparison of the room-temperature spectrum with one taken at 165 eV. This was fitted in an identical manner, the ratio of the two giving the normalization factor. The resulting values for the valence are shown in Fig. 3. The error bars are derived from the variations found in the fit parameters. What is clear from the data, independent of the method used to determine the valence, is that it is constant over the entire temperature range measured.

As a measure of the sensitivity of our method we show in Fig. 6 the spectrum of clean YbGaGe, along with YbGaGe slightly oxidized after some period in the measurement chamber. As expected the contaminated surface shows a small increase in the $4f^{13}$ component whereas the $4f^{12}$ peaks have diminished slightly. The valences for each have been found using the fitting method described above. That of the

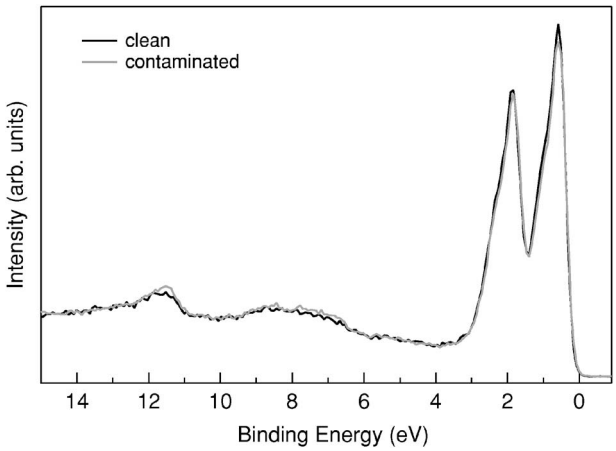

FIG. 6. A comparison of the valence band of clean YbGaGe with that of a slightly oxidized sample, taken with a photon energy of 182 eV.

clean sample is 2.29 whereas the contaminated sample has a valence of 2.32. Thus we are able to distinguish changes in valence down to at least 0.03. This is in agreement with the good sensitivity of photoemission to small changes in valence (see, for example, Refs. 25, 27, and 40).

B. Valence band (high energy)

Figure 7 shows the temperature dependence of the valence band and shallow-core levels measured between 316 K and 121 K with a photon energy of 1421 eV. As mentioned in the Introduction, this photon energy guarantees that the bulk is probed in these measurements: the inelastic electron

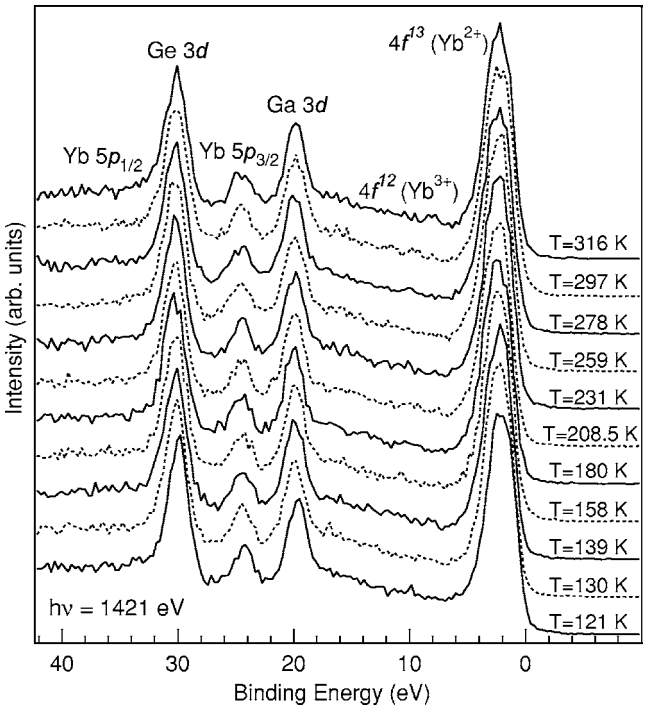

FIG. 7. The valence-band and shallow-core levels of YbGaGe as a function of temperature, measured at a photon energy of 1421 eV.

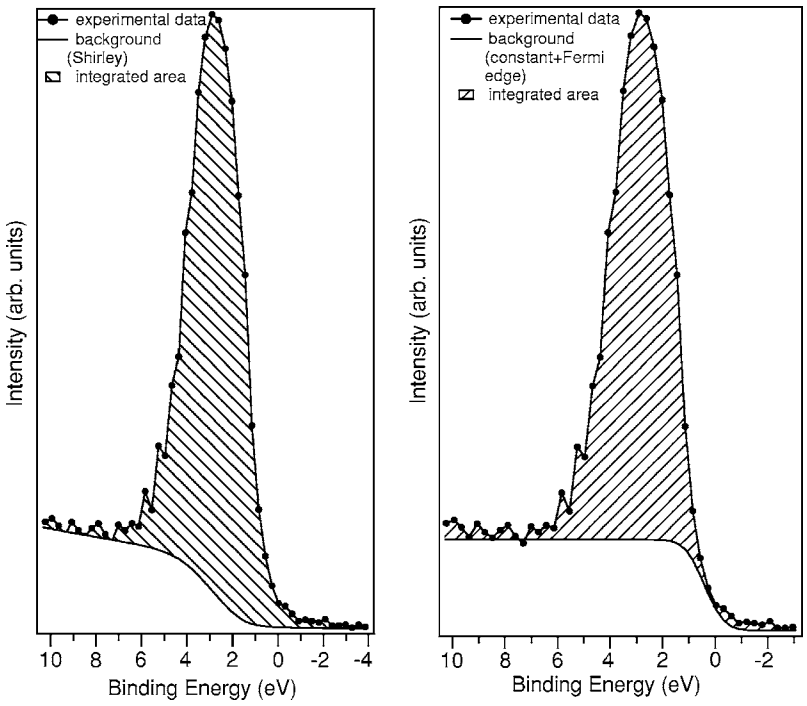

FIG. 8. The two different background subtractions used to determine the Yb^{2+} spectral weight in the valence band when using a photon energy of 1421 eV. The sample temperature was 158 K.

mean free path of valence electrons in YbGaGe at this photon energy is estimated to be about 35 Å as opposed to approximately 10 Å at 182 eV.[41] Our total energy resolution at this energy is not enough to resolve the two $4f^{13}$ components and, without the resonant enhancement present at 182 eV, the $4f^{12}$ features are difficult to discern. The $4f^{13}$ spectral weight was consequently the only one possible to determine by integration after removal of a suitable background. Two different background subtractions were made: the first being a Shirley background taking into account the slope of the valence band before the Yb $4f^{13}$ peak and the second a constant background convoluted with an experimentally broadened Fermi distribution, as suggested by Reinert and coworkers in Ref. 25, which simulates the non-4*f* part of the valence band. The remaining spectrum was integrated to give the $4f^{13}$ spectral weight. Examples of these two background subtraction methods are shown in Fig. 8. In Fig. 9 the values of the Yb $4f^{13}$-integrated intensities thus calculated are plotted. There is no change of the integrated intensity as a function of temperature. This is further proof that there is no Yb valence change from above room temperature down to at least 120 K.

C. Yb 3*d* core level

Figure 10 shows the temperature dependence of the Yb $3d_{5/2}$ photoemission spectra of YbGaGe measured between 297 K and 115 K. The Yb 3*d* core level is split into the $3d_{5/2}$ region at 1515–1545 eV and the $3d_{3/2}$ region at 1560–1590 eV by the spin-orbit interaction.[17,19] We were able to measure only the $3d_{5/2}$ core level because of the limited energy range of the beamline. Comparing the $3d_{5/2}$ spectra of metallic Yb and Yb_2O_3,[18] where the Yb ion is purely divalent or trivalent, respectively, the single peak at 1522 eV can be attributed to Yb^{2+} $3d_{5/2}$ states and the broad small shoulder (whose multiplet structure cannot be resolved due to our experimental resolution), and whose centroid is located at about 1532 eV, can be attributed to the Yb^{3+} $3d_{5/2}$ states. Sato and co-workers[19] demonstrated that valence transitions can be observed monitoring the spectral weights of the 2+ and 3+ components of the Yb 3*d* core level as a function of temperature. In order to do this we have fitted each spectrum with two components having Voigt line shapes, after subtracting an exponential background. We fixed the Gaussian width to be the same for the two components and equal to the total experimental resolution. The Yb $3d_{5/2}$ line shape is seen not to change with temperature from 297 K down to 115 K. We were unable to extrapolate the value for the Yb valence from the Yb 3*d* spectra because of our limited experimental resolution, which broadens the Yb^{3+} $3d_{5/2}$ fine structure, overestimating its spectral weight (and consequently the valence). In Fig. 9 we have plotted the

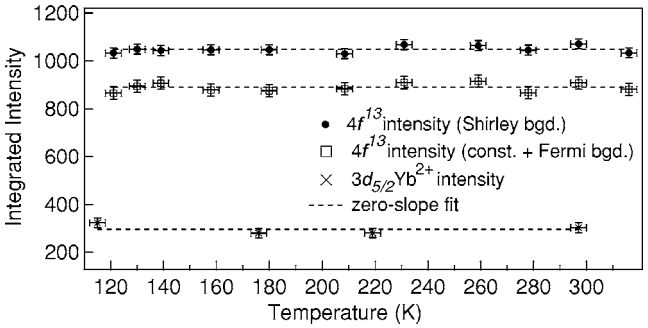

FIG. 9. The intensities, as a function of temperature, for the $4f^{13}$ and $3d_{5/2}$ (2+) parts of the spectrum. The error bars for the $4f^{13}$ intensities have been calculated from the variations in the parameters of the background fits and those for the $3d_{5/2}$ from the variations in the fits of the core level itself. The dashed lines are zero-slope fits to the data.

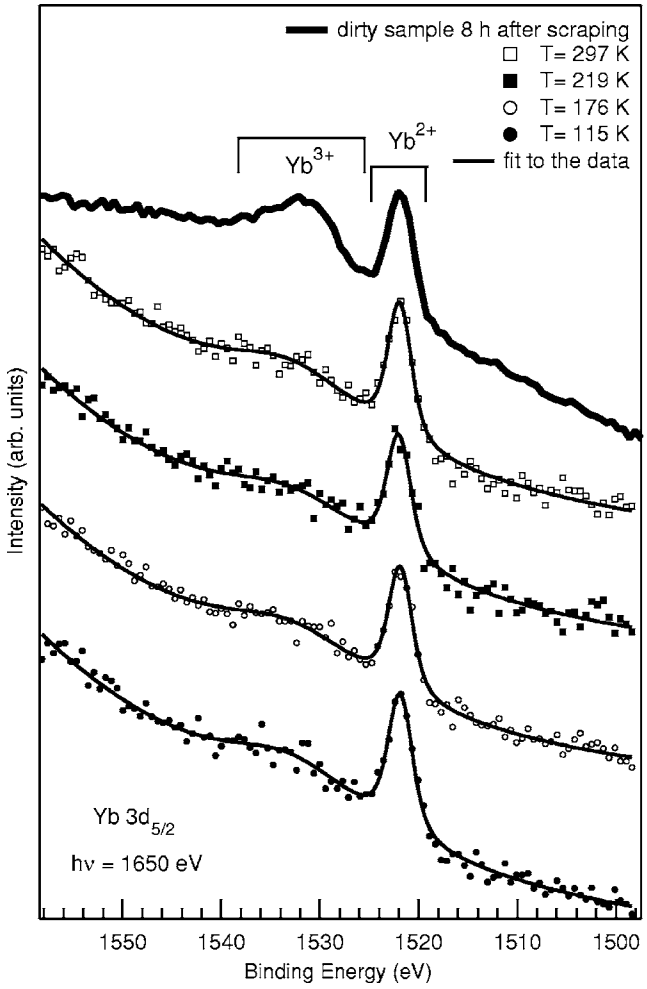

FIG. 10. The Yb $3d_{5/2}$ core level as a function of temperature, taken with a photon energy of 1650 eV, shown together with fits to the experimental data.

value of the Yb^{2+} $3d_{5/2}$ integrated intensity derived from the fit as a function of temperature. As one can see, this value does not change with temperature down to 115 K, within our experimental resolution. As with the valence band spectra, contamination of the surface causes the Yb^{3+} $3d_{5/2}$ component to grow, as shown in the spectrum acquired 8 h after scraping.

D. Yb 4*d* core level

Figure 11 shows the Yb 4*d* core-level photoemission spectrum measured at $T=300$ K, with a photon energy of 1423 eV. The 4*d* structure extends over an energy range of about 30 eV from the main peak. The experimental spectrum is shown together with the spectra for Yb metal (divalent) and oxidized $YbInCu_4$ (trivalent), extracted from Ref. 21. Rare-earth 4*d* photoemission spectra usually exhibit a complex multiplet structure determined by a strong electrostatic interaction (as they have the same principal quantum number), between the 4*d* core hole and the 4*f* unfilled shell. Yb valence strongly affects the Yb 4*d* line shape and binding energy: the clear doublet at 180 eV and 190 eV observed for

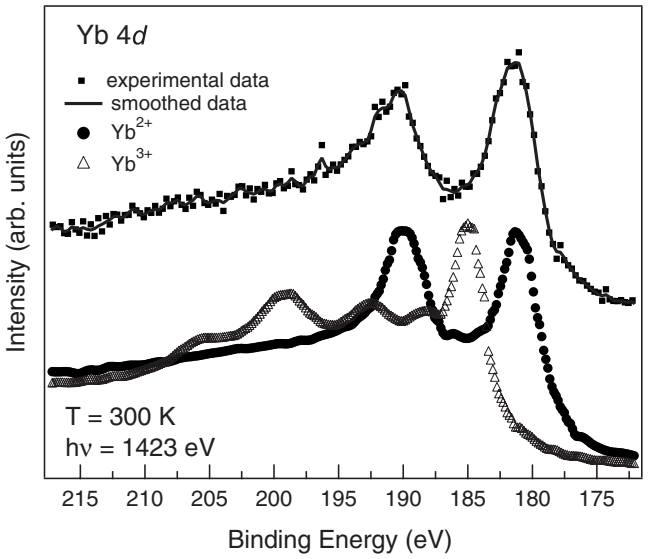

FIG. 11. The Yb 4*d* core level taken at a temperature of 300 K and a photon energy of 1423 eV, shown together with spectra of a divalent and a trivalent compound (see text).

metallic Yb compounds (Yb^{2+}) disappears, replaced by a large peak centered at 185 eV with other less intense components at 188.2 eV, 192.5 eV, 199 eV, and 205.6 eV in oxide-like compounds (Yb^{3+}).[20] These clear changes make the 4*d* core level a clear measure of the valence of Yb. The multiplet intensity and width in our experimental spectrum are very similar to those of metallic Yb (Refs. 20 and 21) and very different from those of nearly trivalent Yb_2O_3 (Ref. 20) or the trivalent oxidized $YbInCu_4$ sample of Schmidt and co-workers.[21] This means that at 300 K Yb ions in YbGaGe have a majority 2+ oxidation state. The main peak at lower binding energy is more intense than that in purely divalent Yb. This is possibly partially due to the presence of the Ge 3*s* core level at the same energy,[42] although the Ge 3*s* cross section at this energy is approximately 11 times less than that of the Yb 4*d*.[43]

IV. DISCUSSION AND CONCLUSIONS

Precise determination of the valence by measurement of the 4*f* levels in the rare earths depends on a precise knowledge of the non-4*f* part of the valence band. It is, however, a reasonable assumption that this non-4*f* contribution is relatively constant with temperature. Furthermore, the large 4*f* cross section at the energies used here[44] discounts the possibility that fluctuations in any other contribution could compensate the much larger 4*f* spectral weight changes that would occur if there was an underlying valence transition. This reasoning applies also to the proposal that the valence transition involves electron transfer to or from the Ga 4*p* band.[3] Apart from the much smaller Ga 4*p* cross section at these energies,[43] any changes in its spectral weight would not be able to uniformly counteract changes in the Yb 4*f* contribution which extends 13 eV into the valence band. Similarly, in the case of the valence band taken at high energy, where only the 2+ spectral weight was measured, the dominant 4*f*

cross section precludes masking of a valence transition by other contributions. Thus, at most, incorrect background subtraction due to incomplete knowledge of the valence band would cause a common shift in the value of the determined valence at all temperatures.

The above discourse does not apply to the Yb $3d_{5/2}$ level which lies in a featureless part of the spectrum. The extracted $3d_{5/2}$ intensity can be taken as an absolute value of the contribution due to the particular valence state.

In Sec. III A we introduced a correction for the on-resonance increase in the Yb^{3+} spectral weight before calculation of the Yb valence. This involved a measurement of the Yb^{3+} spectral weight off-resonance which is low in our case. It follows that any error in its determination could lead to an error in the calculated valences. Such a systematic error would, however, change all the values for the valence equally, leaving our conclusions on the unchanged valence with temperature unaltered.

We have assumed, in the analysis of the low-energy data, that the surface is predominantly divalent. In all probability this assumption is valid, due to the large number of Yb compounds which exhibit this behavior. The presence of a temperature-independent trivalent component in the surface layer would in any case only modify uniformly the value of the valence at all temperatures.

It is known that various Yb systems exhibit $4f^{13}$ peak height changes with temperature, in addition to those due to a change in valence, due to temperature-dependent lattice effects and Fermi functions as well as other factors as explained by Joyce and co-workers in Ref. 24. However, more recently, other Yb systems have been reported where the Yb $4f$ spectrum is unchanged with temperature. In particular high-resolution photoemission measurements which were able to clearly see a valence change as small as from 2.75 to 2.78 in $YbInCu_4$ found no change in the Yb $4f$ spectra for three other related Yb compounds.[40] Thus we do not believe that the YbGaGe system should necessarily show any change, due to non-valence-related effects, with temperature.

It is perhaps pertinent to add that, in their original work, Salvador and co-workers performed valence-bond sum calculations resulting in the two Yb sites possessing valences of 2.0 and 2.6. The value found by us, 2.29 ± 0.015, when fitting the lower-energy data, is almost the exact median of these two values. As the value of the valence found by photoemission is that of the average of the system being measured, our result is perfectly in agreement with those calculations.

As discussed in the Introduction, all subsequent studies have failed to reproduce the ZTE reported in the original work. If indeed it is possible to replicate this effect, the most promising path would appear to be carbon or boron impurity doping, suggested by the possibility of C contamination in the initial study, and which is reported to have led to reduced values for the coefficient of thermal expansion in this compound.[45]

In conclusion, we find no evidence for a valence transition down to almost 100 K in YbGaGe, contrary to the proposal of Salvador and co-workers, but consistent with the majority of work on this system and which casts further doubt on the reported ZTE. We propose that photoemission studies similar to this one will be able to resolve whether valence transitions drive negative thermal expansion in other systems such as $Sm_{2.75}C_{60}$, $Yb_{2.75}C_{60}$, and $Yb_8Ge_3Sb_5$.

Note added in proof. It has been brought to our attention that a recent x-ray absorption study[46] supports our results on the Yb valence behavior in YbGaGe.

ACKNOWLEDGMENTS

We would like to thank Elettra for the provision of the beamtime as a user proposal. A.S.W and A.A.D. would like to thank the Royal Society, the Department of Chemistry UCL, the EPSRC (Grant No. EP/C534654/1), and the ILL for support. Ames Laboratory is operated for the U.S. Department of Energy by Iowa State University under Contract No. W-7405-ENG-82. This work was supported by the Director for Energy Research, Office of Basic Energy Sciences.

*Electronic address: doyle@tasc.infm.it

[1] J. R. Salvador, F. Guo, T. Hogan, and M. G. Kanatzidis, Nature (London) **425**, 702 (2003).
[2] J. R. Salvador, F. Guo, T. Hogan, and M. G. Kanatzidis, Nature (London) **426**, 584(E) (2003).
[3] A. Sleight, Nature (London) **425**, 674 (2003).
[4] A. Jayaraman, E. Bucher, P. D. Dernier, and L. D. Longinotti, Phys. Rev. Lett. **31**, 700 (1973).
[5] J. Arvanitidis *et al.*, Nature (London) **425**, 599 (2003).
[6] S. Margadonna, J. Arvanitidis, K. Papagelis, and K. Prassides, Chem. Mater. **17**, 4474 (2005).
[7] S. Margadonna *et al.*, Chem. Commun. (Cambridge) **2005**, 5754.
[8] Y. Muro *et al.*, J. Phys. Soc. Jpn. **73**, 1450 (2004).
[9] S. Bobev, D. J. Williams, J. D. Thompson, and J. L. Sarrao, Solid State Commun. **131**, 431 (2004).
[10] Y. Janssen *et al.*, J. Alloys Compd. **389**, 10 (2005).
[11] N. Tsujii, T. Furubayashi, H. Kitazawa, and G. Kido, J. Alloys Compd. **393**, 41 (2005).
[12] K.-H. Jang *et al.*, Europhys. Lett. **69**, 88 (2005).
[13] F. R. Drymiotis *et al.*, arXiv:cond-mat/0311584 (unpublished).
[14] S. Margadonna *et al.*, J. Am. Chem. Soc. **126**, 4498 (2004).
[15] U. Burkhardt *et al.* (unpublished).
[16] M. Campagna, G. K. Wertheim, and Y. Baer, in *Photoemission in Solids II: Case Studies*, edited by L. Ley and M. Cardona (Springer-Verlag, Berlin, 1979).
[17] L. Degiorgi *et al.*, Europhys. Lett. **4**, 755 (1987).
[18] F. Patthey and W.-D. Schneider, J. Electron Spectrosc. Relat. Phenom. **81**, 47 (1996).
[19] H. Sato *et al.*, Phys. Rev. Lett. **93**, 246404 (2004).
[20] H. Ogasawara, A. Kotani, and B. T. Thole, Phys. Rev. B **50**, 12332 (1994).
[21] S. Schmidt, S. Hüfner, F. Reinert, and W. Assmus, Phys. Rev. B **71**, 195110 (2005).
[22] L. H. Tjeng *et al.*, Phys. Rev. Lett. **71**, 1419 (1993).

[23] E.-J. Cho *et al.*, Phys. Rev. B **47**, 3933 (1993).
[24] J. J. Joyce, A. B. Andrews, A. J. Arko, R. J. Bartlett, R. I. R. Blyth, C. G. Olson, P. J. Benning, P. C. Canfield, and D. M. Poirier, Phys. Rev. B **54**, 17515 (1996).
[25] F. Reinert, R. Claessen, G. Nicolay, D. Ehm, S. Hufner, W. P. Ellis, G. H. Gweon, J. W. Allen, B. Kindler, and W. Assmus, Phys. Rev. B **58**, 12808 (1998).
[26] J. M. Lawrence, G. H. Kwei, P. C. Canfield, J. G. DeWitt, and A. C. Lawson, Phys. Rev. B **49**, 1627 (1994).
[27] H. Sato *et al.*, Phys. Rev. B **69**, 165101 (2004).
[28] F. Reinert, R. Claessen, G. Nicolay, D. Ehm, S. Hufner, W. P. Ellis, G. H. Gweon, J. W. Allen, B. Kindler, and W. Assmus, Phys. Rev. B **63**, 197102 (2001).
[29] Z. Fisk and J. P. Remeika, in *Handbook on the Physics and Chemistry of Rare Earths*, edited by K. A. Gschneidner, Jr. and L. Eyring (Elsevier, Amsterdam, 1989), Vol. 12.
[30] P. C. Canfield and Z. Fisk, Philos. Mag. B **65**, 1117 (1992).
[31] P. C. Canfield and I. R. Fisher, J. Cryst. Growth **225**, 155 (2001).
[32] Y. Janssen *et al.*, J. Cryst. Growth **285**, 670 (2005).
[33] M. Zangrando *et al.*, Rev. Sci. Instrum. **72**, 1313 (2001).
[34] M. Zangrando *et al.*, Rev. Sci. Instrum. **75**, 31 (2004).
[35] L. I. Johansson, J. W. Allen, I. Lindau, M. H. Hecht, and S. B. M. Hagstrom, Phys. Rev. B **21**, 1408 (1980).
[36] J. W. Allen, in *Synchrotron Radiation Research: Advances in Surface and Interface Science*, edited by R. Z. Bachrach (Plenum Press, New York, 1992), Vol. 1.
[37] D. A. Shirley, Phys. Rev. B **5**, 4709 (1972).
[38] S.-J. Oh, J. W. Allen, M. S. Torikachivili, and M. B. Maple, J. Magn. Magn. Mater. **52**, 183 (1985).
[39] S.-J. Oh, Physica B **186-188**, 26 (1993).
[40] K. Yoshikawa *et al.*, J. Alloys Compd. **408-412**, 92 (2006).
[41] C. J. Powell and A. Jablonski, NIST electron effective-attenuation-length database, version 1.1, National Institute of Standards and Technology, Gaithersburg, MD, 2003.
[42] *Photoemission in Solids I: General Principles*, edited by M. Cardon and L. Ley (Springer-Verlag, Berlin, 1979).
[43] J.-J. Yeh, *Atomic Calculation of Photoionization Cross-Sections and Asymmetry Parameters* (Gordon and Breach, Langhorne, PA, 1993).
[44] J. J. Yeh and I. Lindau, At. Data Nucl. Data Tables **32**, 1 (1985).
[45] F. R. Drymiotis, Y. Lee, G. Lawes, J. C. Lashley, T. Kimura, S. M. Shapiro, A. Migliori, V. Correa, and R. A. Fisher, Phys. Rev. B **71**, 174304 (2005).
[46] C. H. Booth, A. D. Christianson, J. M. Lawrence, L. D. Pham, J. C. Lashley, and F. R. Drymiotis, Phys. Rev. B **75**, 012301 (2007).